

Near-Surface Long-Range Order at the Ordinary Transition: Scaling Analysis and Monte Carlo Results

Peter Czerner and Uwe Ritschel

Fachbereich Physik, Universität GH Essen, 45117 Essen (F R Germany)

Motivated by recent experimental activities on surface critical phenomena, we present a detailed theoretical study of the near-surface behavior of the local order parameter $m(z)$ in Ising-like spin systems. Special attention is paid to the *crossover* regime between “ordinary” and “normal” transition in the three-dimensional semi-infinite Ising model, where a finite magnetic field H_1 is imposed on the surface which itself exhibits a reduced tendency to order spontaneously. As the theoretical foundation, the spatial behavior of $m(z)$ is discussed by means of phenomenological scaling arguments, and a finite-size scaling analysis is performed. Then we present Monte Carlo results for $m(z)$ obtained with the Swendsen-Wang algorithm. In particular the sharp power-law increase of the magnetization, $m(z) \sim H_1 z^{1-\eta_\perp^{ord}}$, predicted for a *small* H_1 by previous work of the authors, is corroborated by the numerical results. The relevance of these findings for experiments on critical adsorption in systems where a small effective surface field occurs is pointed out.

Key words: Surface critical phenomena, critical adsorption, Ising model, Monte Carlo simulation

1 Introduction

A great deal of current experimental activity concentrates on the investigation of critical phenomena near surfaces. After the impressive confirmation of the theoretical predictions [1–4] in experiments with binary alloys [5], the more recent experimental efforts focus on binary mixtures near their consolute point [6–8] and near-critical fluids [9]. In most of these experiments the order parameter, the concentration difference in fluid mixtures or the density difference between liquid and gaseous phase in fluids, plays a central role. For instance the reflectivity and ellipticity measured in light-scattering experiments are directly related to the order-parameter profile [10,11]. Hence,

quantitative information about the local order parameter near the boundary is necessary for the interpretation of the experimental data.

While a very well-developed theory exists for the individual *surface universality classes*, corresponding to fixed point of the renormalization-group flow, the picture in the crossover regions between the fixed points is less complete. The experiments are generically not carried at the fixed points, however, and so a detailed understanding of the crossover region is particularly important.

Consider for example the semi-infinite three-dimensional (3- d) Ising system with spin-spin interaction J . In this model the influence of the surface is usually taken into account by means of a modified exchange interaction J_1 in the surface and a magnetic field H_1 imposed on the surface spins [1,2]. While the former models modifications due to the surface within the critical medium, the latter represents the influence of the adjacent (noncritical) medium, as the container wall for example, on the system.

For a brief (and necessarily incomplete) summary on surface critical phenomena, let us first set $H_1 = 0$. Then at the bulk critical point T_c the tendency to order near the surface can be reduced, increased, or unchanged compared with the bulk. Which case is realized depends on the ratio J_1/J . At a particular value, $J_1^{sp} \simeq 1.5 J$ [1,12,13] the third case is realized. This corresponds to the *surface universality class* of the “special transition”. For $J < J_1^{sp}$ the surface has a reduced tendency to order but nevertheless becomes (passively) ordered at the bulk phase transition. In the opposite case, $J > J_1^{sp}$, the surface orders at a temperature *above* T_c , and *at* T_c the bulk undergoes a phase transition in the presence of an already ordered surface. From the viewpoint of the renormalization group the special transition is an unstable fixed point [2]. For a start value $J_1 < J_1^{sp}$ the (running) surface coupling is driven to the stable fixed point $J_1 = 0$ corresponding to the universality class of the “ordinary transition”. For $J_1 > J_1^{sp}$ it is driven to $J_1 = \infty$, again a stable fixed point, corresponding to the universality class of the “extraordinary transition” [2,14].

Next we consider the effects of H_1 in a system with $J_1 < J_1^{sp}$. This is, for example, the situation generically met in experiments with binary fluids. In particular we are interested in the behavior of the order parameter in this situation. The universality classes are determined by the fixed-point values $H_1 = 0$ and $H_1 = \infty$ of the renormalization-group transformations. For $H_1 = 0$, at the ordinary transition, the order parameter $m(z)$ simply vanishes since, in terms of Ising spins, the symmetry under the reversal $s_i \rightarrow -s_i$ is not broken, neither in the bulk nor in the surface. For $H_1 = \infty$ the universality class is called the “normal transition”. The normal transition is known to be equivalent to the extraordinary transition [15,16]. In both cases $m(z)$ starts from a large m_1 at the surface and then decays to the bulk equilibrium value (being zero for $T \geq T_c$ and nonzero for $T < T_c$). At T_c , i.e. for infinite correlation length ξ , the decay is described by a universal power law $m \sim z^{-\beta/\nu}$ for macroscopic distances z . For instance for the 3- d Ising model $\beta/\nu \simeq 0.52$ [17]. For $T \neq T_c$

a crossover to the exponential decay $\sim \exp(-z/\xi)$ takes place in a distance $z \simeq \xi$ from the surface.

What happens in the crossover region between $H_1 = 0$ and $H_1 = \infty$? Mean-field theory predicts a profile that starts from some finite m_1 and then monotonously decays to the equilibrium value. In Ref. [18] the present authors have shown that, contrary to the naive (mean-field) expectation, fluctuations may cause the order parameter to steeply *increase* to values $m(z) \gg m_1$ in a surface-near regime. This growth is described by a universal power law

$$m(z) \sim H_1 z^\kappa \quad \text{with} \quad \kappa = 1 - n_\perp^{ord}, \quad (1)$$

where η_\perp^{ord} is the anomalous dimension pertaining to the ordinary transition (governing the decay of correlations in the direction perpendicular to the surface [2]). For instance for the 3- d Ising model $\kappa \simeq 0.21$.

The scenario for the crossover between ordinary and normal transition developed in [18] is the following: At bulk criticality and $J_1 < J_1^{sp}$ for any finite H_1 the order-parameter profile increases up to a certain length scale l^{ord} and then crosses over to the power law $\sim z^{-\beta/\nu}$. The scale l^{ord} is given by an *inverse* power of H_1 and, thus, becomes smaller for increasing H_1 such that in the limit $H_1 \rightarrow \infty$ the maximum has moved to the surface. In this limit only the previously mentioned monotonous power-law decay characteristic for the normal transition is left over. A qualitative sketch of typical crossover profiles is shown in Fig. 1. In this plot the axes are logarithmic and both $m(z)$ and z are measured in arbitrary units. The individual curves have the correct asymptotics, $m(z) \sim z^{0.21}$ for $z \rightarrow 0$ and $m(z) \sim z^{-0.52}$ for $z \rightarrow \infty$. However, the (yet unknown) real crossover function is replaced by a simple substitute.

In Ref. [19] it was demonstrated by means of MC simulations and the comparison with exact results that also in the 2- d Ising model the crossover between ordinary and normal transition is qualitatively of the same form as in $d = 3$. However, the simple power law (1) is modified by a logarithm in $d = 2$. The main purpose of the present work is to verify the results for the order parameter obtained in [18], where scaling and heuristic arguments were used and a quantitative calculation in the framework of renormalization-group improved perturbation theory was performed, by means of Monte Carlo (MC) simulation explicitly for the three-dimensional system.

The MC studies devoted to (static) critical phenomena near surfaces that are contained in the literature concentrated mainly on the dependence of thermodynamic variables on J_1/J and, in particular, on critical adsorption for large J_1 [20] as well as on the precise location of J_1^{sp} [13,21]. H_1 was set to zero in these studies. Numerical studies of the influence of H_1 concentrated on the surface layer magnetization [22] and, in the context of wetting, on systems

below the critical temperature [23]. To our knowledge, there is no work in the literature where order-parameter profiles at or above T_c with non-vanishing H_1 were studied by MC methods and which could have been directly compared with the analytic results reported in Ref. [18].

The rest of this paper is organized as follows: In Sec. 2 we summarize and supplement the main results of [18], especially the phenomenological scaling analysis which allows to make quite precise predictions for $m(z)$ in the crossover regime. In Sec. 3 our MC procedure, essentially the Swendsen-Wang algorithm slightly modified to allow for the inclusion of a surface field, is described. The MC results are presented in Sec. 3.3. Eventually, the last section contains besides a short summary remarks on the relevance of our results for experiments.

2 Theory

2.1 Model

We consider the semi-infinite Ising system with a free boundary on a plane square lattice. The exchange coupling between direct neighbors in the bulk is J . In the surface the nearest-neighbor coupling is J_1 . A surface magnetic field H_1 is imposed on the boundary spins and bulk magnetic fields are set to zero

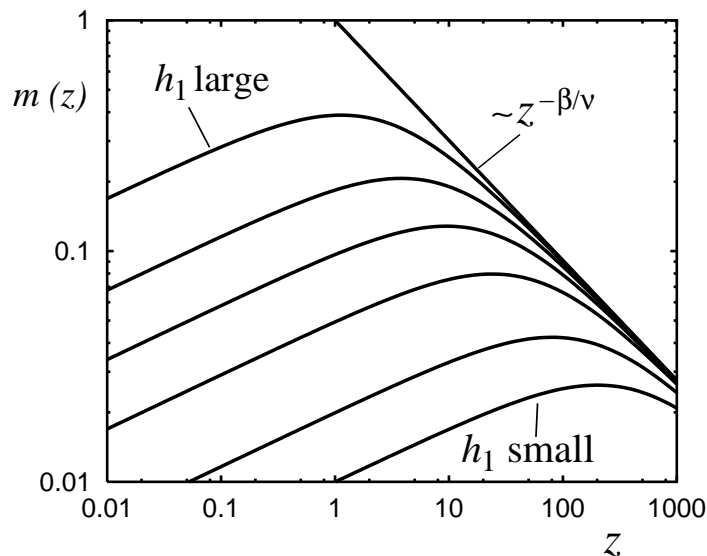


Fig. 1. Qualitative sketch of order-parameter profiles in the crossover regime between ordinary and normal transition in double-logarithmic representation. Both z and m are given in arbitrary units.

such that the Hamiltonian of the model reads

$$\mathcal{H}_{\text{Ising}} = -J \sum_{\langle ij \rangle \in V} s_i s_j - J_1 \sum_{\langle ij \rangle \in \partial V} s_i s_j - H_1 \sum_{i \in \partial V} s_i, \quad (2)$$

where ∂V and V stand for the boundary and the rest of the system (without the boundary), respectively. Below we mainly work with the dimensionless variables

$$K = J/k_B T, \quad K_1 = J_1/k_B T, \quad \text{and} \quad h_1 = H_1/k_B T. \quad (3)$$

For the (reduced) critical bulk coupling we took $K_c \equiv J/k_B T_c = 0.22165$ from the literature [17]. The value of K_1 that corresponds to the special transition is $K_1^{sp} = 1.5 K_c$ [21,13].

2.2 Scaling Analysis

In the critical regime thermodynamic quantities are described by homogeneous functions of the scaling fields. As a consequence, the behavior of the local magnetization under rescaling of distances should be described by

$$m(z, \tau, h_1) \sim b^{-x_\phi} m(zb^{-1}, \tau b^{1/\nu}, h_1 b^{y_1^{ord}}), \quad (4)$$

where $x_\phi = \beta/\nu$ and $y_1^{ord} = \Delta_1^{ord}/\nu$ are the scaling dimensions of the equilibrium magnetization $m(z \rightarrow \infty)$ and the surface field h_1 , respectively [2]. In general the surface exponents have different values for different surface universality scales [2], and so these quantities are additionally marked by ‘*ord*’ for belonging to the ordinary transition. The (MC) literature values for the 3-d Ising model are $x_\phi = 0.518(7)$ [17] and $y_1^{ord} = 0.73$. The value y_1^{ord} was obtained by employing the scaling relation $y_1 + x_1 = d - 1$ together with the recent Monte Carlo result $x_1^{ord} = \beta_1^{ord}/\nu = 1.27$ [24].

Removing the arbitrary rescaling parameter b in Eq. (4) by setting it $\sim z$, one obtains the scaling form of the magnetization

$$m(z, \tau, h_1) \sim z^{-x_\phi} \mathcal{M}(z/\xi, z/l^{ord}), \quad (5)$$

where

$$l^{ord} \sim h_1^{-1/y_1^{ord}} \quad (6)$$

is the length scale determined by the surface field. The second length scale pertinent to the semi-infinite system and occurring in (5) is the bulk correlation length $\xi = \tau^{-\nu}$. Regarding the interpretation of MC data, which are

normally obtained from finite lattices, one has to take into account a third length scale, the characteristic dimension L of the system, and a finite-size scaling analysis has to be performed. The latter will be described in Sec. 2.6.

Going back to the semi-infinite case and setting $\tau = 0$, the only remaining length scale is l^{ord} , and the order-parameter profile can be written in the critical-point scaling form

$$m(z, h_1) \sim z^{-x_\phi} \mathcal{M}_c(z/l^{ord}). \quad (7)$$

As said above, for $z \rightarrow \infty$ the magnetization decays as $\sim z^{-x_\phi}$ and, thus, $\mathcal{M}_c(\zeta)$ should approach a constant for $\zeta \rightarrow \infty$. In order to work out the *short-distance* behavior of the scaling function $\mathcal{M}_c(\zeta)$, we demand that $m(z) \sim m_1$ as $z \rightarrow 0$. This means that in general, in terms of macroscopic quantities, the boundary value of $m(z)$ is *not* m_1 . If the z -dependence of $m(z)$ is described by a power law, it cannot approach any value different from zero or infinity as z goes to zero. However, the somewhat weaker relation symbolized by “ \sim ” should hold, stating that the respective quantity asymptotically (up to constants) “behaves as” or “is proportional to”. This is in accord with and actually motivated by the field-theoretic short-distance expansion [25,2], where operators near a boundary are represented in terms of boundary operators multiplied by c -number functions.

In the case of the 3- d Ising model the foregoing discussion leads to the conclusion that $m(z) \sim h_1$ because the “ordinary” surface with $K_1 < K_1^{sp}$ is paramagnetic and responds linearly to a small magnetic field [15]. This is different in $d = 2$ where an additional logarithmic factor occurs [26], $m_1 \sim h_1 \ln h_1$, and this logarithm also leaves its fingerprint on the near-surface behavior of the magnetization [19].

The immediate consequence of the simple *linear* response in $d = 3$ for the scaling function $\mathcal{M}_c(\zeta)$ occurring in (7) is that it has to behave as $\sim \zeta^{y_1^{ord}}$ in the small- ζ limit. After inserting this in (7), we obtain that the exponent governing the short-distance behavior of $m(z)$ is given by the difference between y_1^{ord} and x_ϕ , such that for $z \ll l^{ord}$ the magnetization is described by

$$m(z) \sim h_1 z^{y_1^{ord} - x_\phi}. \quad (8)$$

Using the scaling relations $\eta_\perp = (\eta + \eta_\parallel)/2$ and $y_1 = (d - \eta_\parallel)/2$ [2], we eventually obtain κ as expressed in (1).

In the mean-field approximation the result for κ is zero. Thus, in this case one really has $m(z \rightarrow 0) = m_1$ and the monotonously decaying order-parameter profile mentioned earlier. However, a positive value is obtained when fluctuations are taken into account below the upper critical dimensionality $d^* = 4$. Taking $y_1^{ord} \simeq 0.73$ from above, the value for κ is 0.21.

Phenomena to some extent analogous to the ones discussed above were reported for the crossover between *special* and normal transition [27]. Also near the special transition the surface field h_1 gives rise to a length scale. However, the respective exponent, the analogy to κ , is negative, and, thus, one encounters a profile that *monotonously* decays for all (macroscopic) z , with different power laws in the short-distance and the long-distance regime and a crossover at distances comparable to the length scale set by h_1 . However, *non-monotonous* behavior in the crossover region as described above for $m(z)$ is a common feature in the case of the energy density in $d = 2$ [28] as well as in higher dimensionality [29].

2.3 Relation to Critical Dynamics

The *spatial* variation of the magnetization discussed so far strongly resembles the *time* dependence of the order parameter in relaxational processes at the critical point. If a system with nonconserved order parameter (model A) is quenched from a high-temperature initial state to the critical point, with a small initial magnetization $m^{(i)}$, the order parameter behaves as $m \sim m^{(i)} t^\theta$ [30], where the short-time exponent θ is governed by the difference between the scaling dimensions of initial and equilibrium magnetization divided by the dynamic (equilibrium) exponent [31]. Like the exponent κ in (1), the exponent θ vanishes in MF theory, but becomes positive below d^* . For example, its value in the 3- d Ising model with Glauber dynamics is $\theta = 0.108$ [32].

The high-temperature initial state of the relaxational process is to some extent analogous to the surface that strongly disfavors the order and that (for $h_1 = 0$) belongs to the universality class of the ordinary transition. Further expanding this analogy, heating a system from a low-temperature (ordered) initial state to the critical point would be similar to the situation at the extraordinary transition. Eventually, analogous to the special transition would be a “relaxation process” that starts from an equilibrium state at T_c .

2.4 Heuristic Argument

There is also a heuristic argument for the growth of the magnetization in the near-surface regime expressed in (1). As said above, a small h_1 generates a surface magnetization $m_1 \sim h_1$. Regions that are close to the surface will respond to this surface magnetization by ordering as well. How strong this influence is depends on two factors.

First, it is proportional to the correlated area in a plane parallel to the surface at a distance z . While correlations in the surface are asymptotically (for $J_1 \rightarrow 0$) suppressed, for $z > 0$ the range of correlations between spins located in a

plane parallel to the surface in a distance ρ from each other can be regarded as finite, because for $\rho > z$ the parallel correlation function is governed by surface exponents and decays much faster than in the bulk. Hence the corresponding effective correlation length, $\xi_{\parallel}(z)$, should behave as z . Referring once more to critical dynamics as discussed in the previous section, $\xi_{\parallel}(z)$ is analogous to the time dependent (growing) correlation length $\xi(t) \sim t^{1/\zeta}$ (where ζ here stands for the dynamic equilibrium exponent).

Second, it depends on the probability that a given spin orientation has “survived” in a distance z . For small h_1 and $z < l^{ord}$, the latter is governed by the *perpendicular* correlation function $C(z) \sim z^{-(d-2+\eta_{\parallel}^{ord})}$. Taking into account both factors, we obtain

$$m(z) \sim h_1 C(z) \xi_{\parallel}^{d-1} = h_1 z^{1-\eta_{\perp}^{ord}}, \quad (9)$$

the short-distance power law reported in (1). Qualitatively speaking, the surface when carrying a small m_1 induces a much larger magnetization in the adjacent layers, which are much more susceptible and capable of responding with a magnetization $m \gg m_1$.

This simple picture for the anomalous short-distance behavior holds for dimensions $2 < d < 4$. At and above the the upper critical dimension $d^* = 4$, where the mean-field theory starts to provide the correct description, the power-law growth of magnetization is not observed, since there the increase of the correlated surface area is compensated by the decay of the perpendicular correlation function. In the case of the two-dimensional Ising model the assumption that $m_1 \sim h_1$ is no longer valid, and logarithmic terms occur [19].

2.5 Modifications at $T \neq T_c$

The phenomenological scaling analysis presented above can be straightforwardly extended to the case $\tau > 0$. In $d > 2$, we may assume that the behavior near the surface for $z \ll \xi$ is unchanged compared to (1), and, thus, the increasing profiles are also expected slightly above the critical temperature. The behavior farther away from the surface depends on the ratio l^{ord}/ξ . In the case of $l^{ord} > \xi$ a crossover to an exponential decay will take place for $z \simeq \xi$ and the regime of nonlinear decay does not occur. For $l^{ord} < \xi$ a crossover to the power-law decay $\sim z^{-\beta/\nu}$ takes place and finally at $z \simeq \xi$ the exponential behavior sets in.

An interesting phenomenon can be observed in the case $\xi < l^{ord}$. As discussed above, $m(z)$ then never reaches the regime with power-law decay, but crosses over from the near-surface increase directly to the exponential decay. Since the region where $m(z)$ grows extends up to the distance ξ , the magnetization

in the maximum has roughly the value $m_{max} \simeq \xi^\kappa$. Now, the amplitude of the exponential decay should behave as $\sim m_{max}$ such that for $z \gg \xi$ we have

$$m(z) \sim h_1 \xi^\kappa \exp(-z/\xi). \quad (10)$$

In other words, in the case $\xi < l^{ord}$ the short-distance exponent κ not only governs the behavior of $m(z)$ near the surface, but also leaves its fingerprint much farther away from the surface in form of an universal dependence of the *amplitude* of the exponential decay on the correlation length $\sim \xi^\kappa$. Nothing comparable occurs when $\xi = \infty$ (compare Sec. 2.2 above). When l^{ord} is the only scale, all profiles approach the same curve $m(z) \approx \mathcal{A} z^{-\beta/\nu}$ for $z \gtrsim l^{ord}$, with an amplitude \mathcal{A} *independent* of h_1 . An analogous phenomenon, termed “long-time memory” of the initial condition, does also occur in critical dynamics for $T \geq T_c$ [33].

Below the critical temperature (and near the ordinary transition), the short-distance behavior of the order parameter is also described by a power law, this time governed by a different exponent, however [34]. The essential point is that below T_c the surface orders spontaneously even for $h_1 = 0$. Hence, in the scaling analysis the scaling dimension of h_1 has to be replaced by the scaling dimension of m_1 , the conjugate density to h_1 , given by $x_1^{ord} = \beta_1^{ord}/\nu$ [2]. The exponent that describes the increase of the profile is thus $x_1^{ord} - x_\phi$ [34], a number that even in mean-field theory is different from zero ($= 1$) and for the $3 - d$ Ising model its value is 0.75.

2.6 Finite Size Scaling

In order to assess the finite size effects to be expected in the MC simulations, we have to take into account the finite-size length scale L . The latter is proportional to the linear extension of the lattice (called N below). The generalization of (4) reads [35]

$$m(z, \tau, h_1, L) \sim b^{-x_\phi} m(zb^{-1}, \tau b^{1/\nu}, h_1 b^{y_1^{ord}}, Lb^{-1}), \quad (11)$$

and proceeding as before, we obtain as the generalization of (5) to a system of finite size:

$$m(z, \tau, h_1, L) \sim z^{-x_\phi} \mathcal{M}(z/\xi, z/l^{ord}, z/L). \quad (12)$$

Thus even at T_c there are two macroscopic length scales, on the one hand L (imposed by the geometry) and on the other hand l^{ord} (the scale set by h_1).

It is well known that for large $z \gtrsim L$ we have to expect an exponential decay of $m(z)$ on the scale L . In the opposite limit, when z is smaller than both L and

l^{ord} , we expect the short-distance behavior (1) to occur. That this expectation turns out to be correct is the necessary condition for observing (1) in MC simulations. Stated in terms of correlation lengths it means that as long as $\xi_{||}$ (cf. discussion in Sec. 2.4) is smaller than L (and the bulk correlation length ξ), the form of the profile is unchanged compared to the one of the semi-infinite system (at bulk criticality). In particular it implies that the surface magnetization m_1 , whose linear response to h_1 was an important ingredient to our scaling analysis of Sec. 2.2, should not depend on L , as long as L can be regarded as macroscopic.

Farther away from the surface, the form of the profile depends on the ratio between l^{ord} and L . In the case of $l^{ord} > L$ a crossover to an exponential decay will take place for $z \simeq L$, and, analogous to the situation with a finite correlation length, also in the finite-size system the amplitude of this exponential decay is governed by the exponent κ (compare to (10) and the discussion in Sec. 2.3), such that we have for $z \gg L$

$$m(z) \sim h_1 L^\kappa \exp(-z/L) \quad (13)$$

Again, analogous finite-size effects were reported also in relaxation processes near criticality [33]. In the opposite case, $l^{ord} < L$, a crossover to the power-law decay $\sim z^{-x_\phi}$ takes place, followed by the crossover to the exponential behavior at $z \simeq L$. Thus, qualitatively, the discussion for systems of finite size is largely analogous to the one in Sec. 2.3 for finite ξ .

3 Monte Carlo Simulation

3.1 System

The results of the scaling analysis, especially the short-distance law (1), were checked by MC simulations. To this end we calculated order-parameter profiles for the 3- d Ising model with uniform bulk exchange coupling K and set $K_1 = 0$, corresponding to the fixed-point value of the ordinary transition.

The geometry of the systems studied was that of a rectangular (cuboidal) lattice with two free surfaces opposite to each other and the other boundaries periodically coupled. The surface field h_1 was imposed on both free surfaces. The linear dimension perpendicular to the surfaces was taken to be two times larger than the lateral extension in order to keep corrections due to the second surface, the so-called Fisher-de Gennes effect [36], small [36]. Hence, when we talk about a lattice of size N in this section, we refer to a rectangular system with $N^2 \times 2N$ spins.

The distance from the surface is still called z in the following, although it is clearly an integer quantity, with $z = 0$ corresponding to the location of one of the surfaces. Order parameter profiles were calculated by averaging in individual configurations over planes parallel to the surface and, in turn, we averaged over a large number of configurations generated by the algorithm described in Sec. 3.2. Eventually the symmetry of the system was used and also the average between the left and right half of the lattice was taken.

3.2 Procedure

We consider the Ising model, defined by (2). The aim of the (equilibrium) Monte Carlo procedure is to generate a representative sample of configurations \mathbf{s} distributed according to the Boltzmann factor $P(\mathbf{s}) \sim \exp[\mathcal{H}(\mathbf{s})/k_B T]$ [37]. Further, it must be guaranteed that, starting from any initial configurations, after a reasonable amount of time such a sample can be extracted. The latter is in principle provided if the algorithm that generates a new configuration \mathbf{s}' from the old one satisfies *detailed balance*. In terms of transition probabilities $W(\mathbf{s} \rightarrow \mathbf{s}')$ this condition can be expressed as

$$W(\mathbf{s} \rightarrow \mathbf{s}') \exp[-\mathcal{H}(\mathbf{s})/k_B T] = W(\mathbf{s}' \rightarrow \mathbf{s}) \exp[-\mathcal{H}(\mathbf{s}')/k_B T] . \quad (14)$$

For practical purposes, however, not any algorithm satisfying (14) is suitable for MC simulations of critical or near-critical systems. The reason is that physically meaningful algorithms, like Glauber and Kawasaki dynamics [37], are greatly hampered by the *critical slowing down* upon approaching the equilibrium. One way out of this dilemma is the Swendsen-Wang (SW) algorithm [38], which satisfies (14) but does (probably) not correspond to a physically meaningful dynamics.

The SW algorithm generates a transition (or update) $\mathbf{s} \rightarrow \mathbf{s}'$ between spin configurations via connected bond clusters. A cluster configuration \mathbf{n} is constructed from \mathbf{s} by creating bonds between neighboring spins of *equal* sign. Then these bonds are “activated” [39] with probability

$$p = 1 - e^{-2K} . \quad (15)$$

No bonds are generated between spins of *opposite* sign. As the next step, bond clusters are defined as connected sets of active bonds. Also isolated spins are identified as a cluster, such that eventually each spin belongs to a cluster.

In order to obtain a new spin configuration \mathbf{s}' from \mathbf{n} , one assigns to all sites of a given cluster a new spin value with equal probability for each spin direction (independent of the old spin value). The probability for the transition $\mathbf{s} \rightarrow \mathbf{s}'$

$$W(\mathbf{s}|\mathbf{n}|\mathbf{s}') = p^b (1-p)^m q^{-N_c} \quad (16)$$

where \mathbf{n} is an intermediate cluster configuration with N_c clusters, and b and m are the numbers of “active” and “inactive” bonds, respectively. This transition corresponds to one Monte Carlo sweep.

In order to verify that the algorithm satisfies detailed balance, we have to consider a transition in the opposite direction. For the transition \mathbf{s}' from \mathbf{s} via the *same* cluster configuration \mathbf{n} , there is a probability

$$W(\mathbf{s}|\mathbf{n}|\mathbf{s}') = p^b(1-p)^{m'}q^{-N_c}, \quad (17)$$

with the same b and N_c as before. However, the number of non-active bonds m' can in general be different, because neighboring clusters can originate from domains with spins of the same or of different sign, in both cases leading to the same cluster configuration.

The total transition probability from \mathbf{s} to \mathbf{s}' is given by

$$W(\mathbf{s}, \mathbf{s}') = \sum_{\mathbf{n}} W(\mathbf{s}|\mathbf{n}|\mathbf{s}'), \quad (18)$$

where the sum runs over all possible intermediate cluster configurations \mathbf{n} . Since the sum $b + m$ is constant for a given spin configuration, it is straightforward to show that

$$\frac{W(\mathbf{s} \rightarrow \mathbf{s}')}{W(\mathbf{s}' \rightarrow \mathbf{s})} = (1-p)^{m-m'}. \quad (19)$$

Eventually, taking into account that the energy difference between \mathbf{s} and \mathbf{s}' is given by

$$-2J(m - m') = -\Delta\mathcal{H}, \quad (20)$$

with (15) one obtains the detailed balance relation (14).

The algorithm presented so far works as long as no magnetic fields are imposed on the spins. To take into account the third term in (2) that describes the influence of the surface magnetic field H_1 , we follow Wang [40] and introduce a layer of “ghost” spins next to the surface that couple to the surface spins only. The “ghost” spins all point in the direction of H_1 and couple to the “real” spins with coupling strength equal to H_1 . If one or more “active” bond between a surface and a ghost spin exist, the cluster has to keep its old spin when the system is updated. This prescription preserves detailed balance. In the practical calculation this rule was realized by a modified (reduced) spin-flip probability

$$p(n_s) = 1 - \frac{1}{2} \exp(-2 h_1 n_s) \quad (21)$$

for clusters pointing in the direction of h_1 , where n_s is the number of *surface* spins contained in the cluster. For clusters pointing in opposite direction the probability has to remain unchanged (equal to $1/2$).

In order to obtain an equilibrium sample, we discarded several hundred – the precise number depended on the size of the system – configurations after the start of the run. To keep memory consumption low, we used multispin-coding techniques, i.e. groups of 64 spins were coded in one long integer. All calculations were run on a Silicon Graphics computer (Power Challenge) with four Risk 8000 processors. To obtain a profile with reasonable statistics for our largest system ($N=256$) took about one week of (single-processor) CPU time.

3.3 Results

From the magnetization profiles especially the surface magnetization m_1 as a function of h_1 can be extracted. It is instructive to compare the results for the 3- d Ising model with those for the two-dimensional case obtained in Ref. [19]. This is done in Fig. 2. The crosses represent the data obtained from a three-dimensional system with $N = 256$, the circles stem from the two-dimensional Ising model with lattice size 512×2048 . In both cases the statistical errors are smaller than the symbol size.

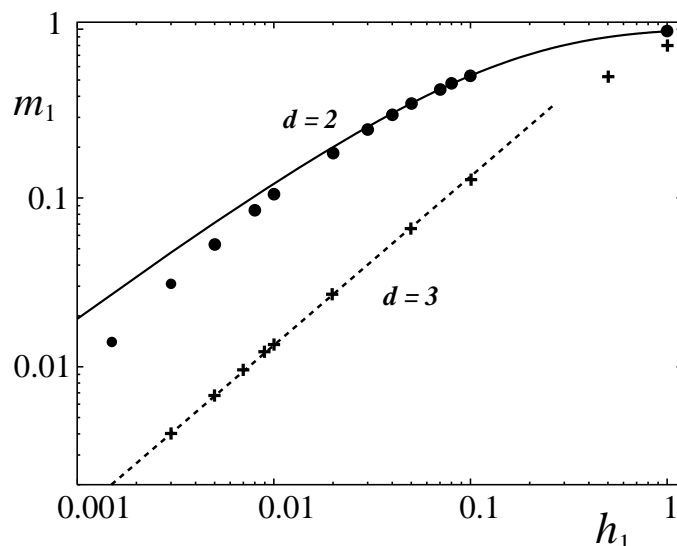


Fig. 2. Surface magnetization m_1 as a function of h_1 for the Ising model in $d = 2$ (full circles) and $d = 3$ (crosses) in double-logarithmic representation. The data for $d = 2$ stem from a 512×2048 lattice, those for $d = 3$ from a $256^2 \times 512$ system. The solid line shows the exact result for the $d = 2$ semi-infinite system. The dashed line is a fit to the our MC data.

The situation in three dimensions is obviously quite simple. Up to $h_1 \simeq 0.1$ the response of m_1 on h_1 is just linear. This is the regime where the scaling analysis of Sec. 2.2 applies, in particular the basic assumption that $m(z) \sim h_1$ as z goes to zero. The dashed line is a linear fit to the data for $h_1 \leq 0.1$. For larger values of h_1 the surface magnetization saturates, such that for $h_1 \rightarrow \infty$ the curve has to approach unity

The dependence of m_1 on the surface field in two dimensions is more complicated. As discussed in detail in Ref. [19] and investigated in many exact calculations [26], there occurs a logarithmic factor in the functional dependence of m_1 on h_1 . The solid line shows the exact result of the semi-infinite system, which, due to the logarithm, never goes through a regime of linear behavior. The MC data (see Ref. [19]) deviate from the exact curve for $h_1 \lesssim 0.02$ and for small h_1 indeed show a linear dependence. This observation, linear response for small h_1 and an approach to the true semi-infinite behavior for larger h_1 , is a finite-size effect consistent with exact results [26].

The next point are finite-size effects in the vicinity of the surface, especially concerning the dependence of m_1 on N . As discussed in Sec. 2.6, we expect that m_1 and the profile up to a certain distance $\sim N$ should not depend on N . In Fig. 3 we plotted the data for the local magnetization for four different system sizes ranging from $N = 64$ to 256 up to $z = 20$. In all cases the surface field was $h_1 = 0.01$. Quite obviously, m_1 itself does not vary with N in the given range of sizes, confirming the finite-size scaling analysis in Sec. 2.6 as well as the assumptions underlying the scaling analysis in Sec. 2.2. From the given value of m_1 all profiles increase for z increasing away from the surface. For the first few layers the curves lie on top of each other, but in the smaller systems the slopes become smaller compared to larger N at relatively small distances already. For the system with $64^2 \times 128$ spins the regime with growing magnetization extends to $z \simeq 7$ only.

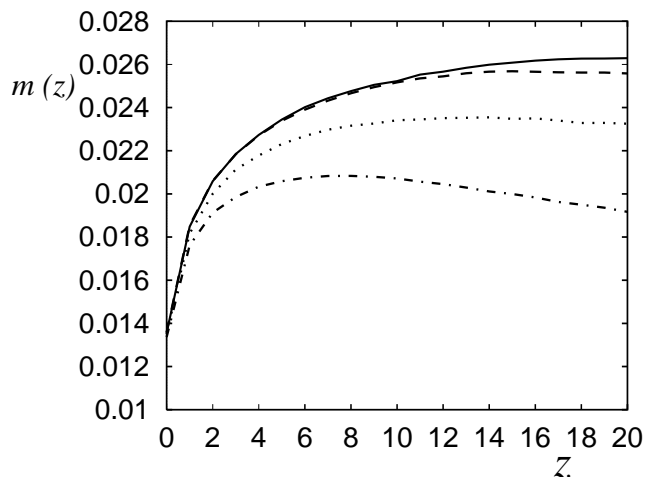


Fig. 3. The local magnetization at and in the immediate vicinity of the surface for $h_1 = 0.005$ and $N = 64$ (dashed-dotted), 128 (dotted), 196 (dashed), and 256 (solid line).

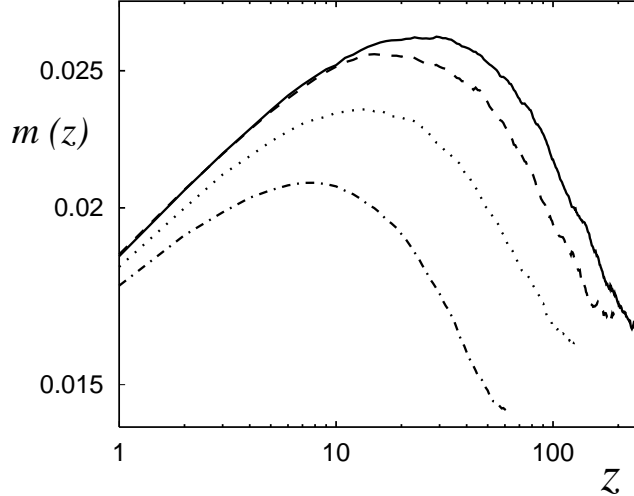


Fig. 4. Order-parameter profiles for the same parameters as in Fig.3 in double-logarithmic representation.

The variation of the same curves on larger scales is displayed in Fig.4 in double-logarithmic form. Going to larger system size the distance of the maximum z_{max} grows roughly as $\sim N$. For $N = 256$ we have $z_{max} \simeq 30$. Recalling the results of the finite-size scaling analysis of Sec.2.6, we conclude that with these parameters the model is in the regime where $L < l^{ord}$, and going to a smaller h_1 that would increase l^{ord} would not help to extend the region of growing magnetization. For $z \rightarrow 0$ the form of the profiles is consistent with a power law. However, in the small systems the finite size effects cause the profiles to crossover to the exponential decay (compare Sec.2.6) at a rather small distance. Even in the largest system $N = 256$ that could be studied by our present means with reasonable effort, the near-surface power law does not extend beyond $z \simeq 20$. The problem is that we indeed have $L \sim N$, but apparently with a rather small constant of proportionality.

Nevertheless a rough value for the short-distance exponent can be extracted from the profile for $N = 256$. The result is $\kappa = 0.16(2)$. This is somewhat lower than our expectation. The deviation from the expected value 0.21 is very likely due to the finite-size effects. We can not claim to see the power law (1) over a really macroscopic range before the crossover to the finite-size (exponential) behavior sets in. So the determination of a more reliable value of κ from the short-distance behavior remains as a task for larger-scale simulations.

Magnetization profiles for $N = 256$ and h_1 varying in a wide range between 0.005 and 5 are plotted in Fig. 5. The dashed line represents the pure power law $\sim z^{-0.52}$ characteristic for the extraordinary or normal transition. For small h_1 , up to $h_1 \simeq 0.1$, the curves show the near-surface growth consistent with (1). For h_1 up to about 0.02, the location of the maximum (here $z_{max} \simeq 30$) is determined by the finite-size scale L . Setting h_1 to larger values, the maximum moves closer to the surface. This is the regime where l^{ord} is smaller than L and the location of the maximum is governed by l^{ord} . In the case of $h_1 \gtrsim 0.2$,

the profiles decay monotonously. Setting $h_1 = 5.0$, the magnetization at the surface is very close to one, and the decay for $10 \lesssim z \lesssim 100$ is consistent with the power law $\sim z^{-x_\phi}$. The value of the exponent $x_\phi = \beta/\nu$ obtained from this curve is 0.51(1), which is in excellent agreement with the literature value 0.517 [17]. The up-bending of the profiles for $z \gtrsim 100$ is due to the second surface.

Eventually, Fig. 6 shows the values of z_{max} as a function of h_1 determined from the profiles of Fig. 5. From these data, the qualitative picture from above can be made more quantitative. Especially with the result Eq. (6) we can in principle determine directly the scaling dimension y_1^{ord} . A power law fitted to the data for $0.02 \leq h_1 \leq 0.1$ yields $1/y_1^{ord} = 1.4(1)$ (where the error was

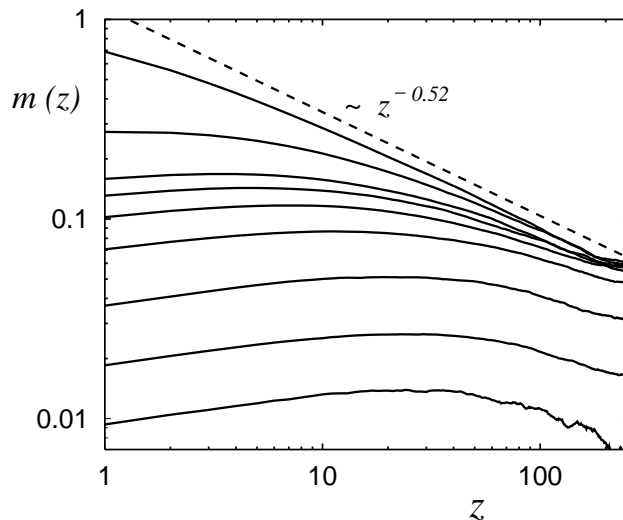


Fig. 5. Order-parameter profiles for $N = 256$ and $h_1 = 0.005, 0.01, 0.02, 0.04, 0.08, 0.1, 0.2$, and 5.0 in double-logarithmic representation. The pure power law $\sim z^{-0.52}$ (dashed line) is shown for comparison.

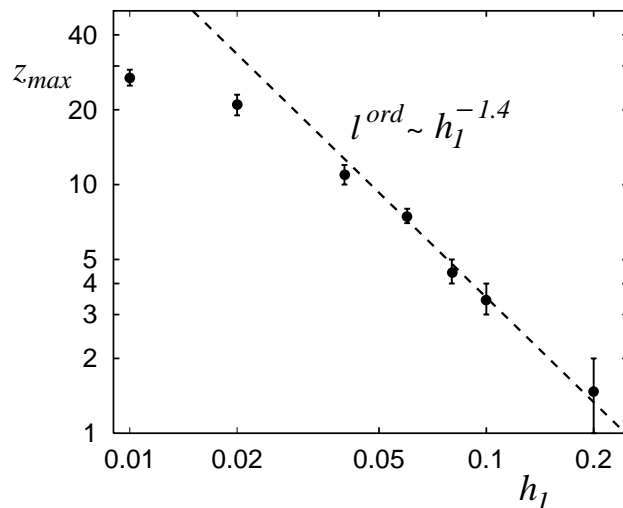


Fig. 6. z_{max} in dependence of h_1 in double-logarithmic representation as obtained from the profiles of Fig. 5. The error bars were estimated. The dashed line depicts the derived power-law dependence of the length scale l^{ord} on h_1 .

estimated), which, in turn, yields 0.71(4) for the scaling dimension y_1^{ord} . As mentioned above the literature value is 0.73. However, as in the case of the short-distance exponent, we also here have to admit that we are not really in a regime where we can call l^{ord} large compared with the lattice spacing, and the good agreement with what we expected from the scaling analysis is actually surprising.

4 Summary and Concluding Remarks

We studied the near-surface behavior of the order parameter in the three-dimensional Ising system under the influence of a surface magnetic field H_1 . The anomalous behavior found in [18] by employing scaling arguments and perturbative methods was confirmed in the present work by Monte Carlo simulations. Especially, the short-distance power law (1) was corroborated.

However, in our Monte Carlo study especially the region with small H_1 is severely affected by finite size effects. Even in our largest system ($256^2 \times 512$) the increase of $m(z)$ does not extend beyond $z \simeq 30$. In order to obtain reliable results for the exponent κ determined with the help of the short-distance power law (1) and profiles that can be used for the quantitative comparison with experimental data, one has to go to systems beyond the size that we are able to treat by our present means.

Concerning experiments on surface critical phenomena, our results should be of interest especially in those cases where a small H_1 occurs, at a surface that disfavors the order. An example where this was obviously realized is the system studied by Desai et al. [8]. In their experiment a binary fluid was studied in a container whose walls as a function of time change their preference from one component to the other, the time scale of this change being of the order of days. In other words, the surface field H_1 changes sign as time goes by, and during a certain period H_1 is small. First substantial steps towards a theoretical explanation of this and other similar experiments on binary mixtures were made already by Ciach et al. [41]. A complete theoretical analysis would require a careful derivation of experimentally observable quantities like reflectivity and ellipticity for light scattering experiments on the basis of our results for the order-parameter profile.

Another experiment, discussed already in some detail in [18], is the one by Mailänder et al. [5] on Fe_3Al . This system undergoes (among other transitions) a second-order phase transition between a phase with DO_3 structure and one with $B2$ structure. The near-surface regime was studied by scattering of evanescent x-rays. The exponents observed were consistent with the expectation for the ordinary transition, but Bragg peaks revealed the existence of long-range order near the surface reminiscent to the normal transition. In

order to explain the experimental results of [5] on the basis of our findings we have to assume that there exists an effective H_1 in this system. Then, if the associated length scale l^{ord} is larger than both the scattering depth and the bulk correlation length, the structure function is governed by the anomalous dimension of the ordinary transition. On the other hand, the steep increase of the order parameter should provide the explanation for the observed long-range order near the surface.

Acknowledgements: We thank A. Ciach for helpful comments and discussions. We are especially indebted to our system administrator R. Oberhage for his professional support concerning computer questions. This work was supported in part by the Deutsche Forschungsgemeinschaft through Sonderforschungsbereich 237.

References

- [1] For reviews on surface critical phenomena see K. Binder, in *Phase Transitions and Critical Phenomena*, Vol. 8, C. Domb and J. L. Lebowitz, eds. (London, Academic Press, 1983) and Ref. [2].
- [2] H. W. Diehl, in *Phase Transitions and Critical Phenomena*, Vol. 10, C. Domb and J. L. Lebowitz, eds. (London, Academic Press, 1986).
- [3] H. W. Diehl and S. Dietrich, Z. Phys. B **42**, 65 (1981); Erratum B **43** (1981) 281.
- [4] S. Dietrich and H. Wagner, Phys. Rev. Lett. **51** (1983) 1469; Z. Phys. B **56** (1984) 207.
- [5] X. Mailänder, H. Dosch, J. Peisl, and R. L. Johnson, Phys. Rev. Lett. **64** (1990) 2527; see also: H. Dosch, in *Critical Phenomena at Surfaces and Interfaces, Springer Tracts in Modern Physics*, edited by G. Höhler and E. A. Niekisch, (Springer, Berlin, 1992).
- [6] B. M. Law, Phys. Rev. Lett. **67** (1991) 1555; C. L. Caylor and B. M. Law, J. Chem. Phys. **104** (1996) 2070; S. P. Smith and B. M. Law, Phys. Rev. E **52** (1996) 580.
- [7] Hong Zhao, A. Penninckx-Sans, Lay-Theng Lee, D. Beysens, and G. Jannink, Phys. Rev. Lett. **75** (1995) 1977.
- [8] N. S. Desai, S. Peach, and C. Franck, Phys. Rev. E **52** (1995) 4129.
- [9] S. Blümel and G. H. Findenegg, Phys. Rev. Lett. **54** (1985) 447; M. Thommes and G. H. Findenegg, Adv. in Space Res. **16** (1995) 83.
- [10] M. Schlossmann, X.-L. Wu, and C. Franck, Phys. Rev. B **31** (1985) 1478; J. A. Dixon, M. Schlossmann, X.-L. Wu, and C. Franck, Phys. Rev. B **31** (1985) 1509.
- [11] B. M. Law and D. Beaglehole, J. Phys. D **14** (1981) 115.

- [12] D. P. Landau and K. Binder, Phys. Rev. B **41** (1990) 4633.
- [13] C. Ruge, S. Dunkelmann, and F. Wagner, Phys. Rev. Lett. **69** (1992) 2465; C. Ruge, S. Dunkelmann, F. Wagner, and J. Wulf J. Stat. Phys. **73** (1993) 293.
- [14] M. Smock and H. W. Diehl, Phys. Rev. B **47** (1993) 5841.
- [15] A. J. Bray and M. A. Moore, J. Phys. A **10** (1977) 1927.
- [16] H. W. Diehl and T. W. Burkhardt, Phys. Rev. B **50** (1994) 3894.
- [17] A. M. Ferrenberg and D. P. Landau, Phys. Rev. B **44** (1991) 5081.
- [18] U. Ritschel and P. Czerner, *Near-surface long-range order at the ordinary transition*, Essen preprint (1996).
- [19] P. Czerner and U. Ritschel, *Magnetization Profile in the $d=2$ Semi-Infinite Ising Model and Crossover between Ordinary and Normal Transition*, Essen preprint (1996).
- [20] D. P. Landau and K. Binder, Phys. Rev. B **41** (1990) 4786; M. Smock, H. W. Diehl, and D. P. Landau, Ber. Bunsenges. Phys. Chem. **98** (1994) 486.
- [21] K. Binder and D. P. Landau, Phys. Rev. Lett. **52** (1984) 318.
- [22] K. Binder and D. P. Landau, Physica A **163** (1990) 17.
- [23] K. Binder and D. P. Landau, Phys. Rev. B **37** (1988) 1745; Phys. Rev. B **46** (1992) 4844; K. Binder, D. P. Landau and S. Wansleben, Phys. Rev. B **40** (1989) 6971.
- [24] C. Ruge, *Critical Exponents and Universal Amplitude Ratios for the $d = 3$ Ising Model with Surfaces*, doctoral thesis (Kiel 1994).
- [25] K. Symanzyk, Nucl. Phys. B **190** [FS3] (1981) 1; H. W. Diehl and S. Dietrich, Z. Phys. B **42** (1981) 65.
- [26] H. Au-Yang, J. Math. Phys. **14** (1973) 937; H. Au-Yang and M. E. Fisher, Phys. Rev. B **21** (1980) 3956.
- [27] E. Brézin and S. Leibler, Phys. Rev. B **27** (1983) 594; A. Ciach and H. W. Diehl, (unpublished).
- [28] L. V. Mikheev and M. S. Fisher, Phys. Rev. B **49** (1994) 378.
- [29] E. Eisenriegler, J. Chem. Phys. **79** (1983) 1052; E. Eisenriegler, M. Krech, and S. Dietrich, Phys. Rev. B **53** (1996) 14377;
- [30] H. K. Janssen, B. Schaub, and B. Schmittmann, Z. Phys. B **73** (1989) 539.
- [31] H. W. Diehl and U. Ritschel, J. Stat. Phys. **73** (1993) 1; U. Ritschel and H. W. Diehl, Nucl. Phys. B **464** (1996) 512.
- [32] Z.-B. Li, U. Ritschel and B. Zheng, J. Phys. A: Math. Gen. **27** (1994) L837 ; P. Grassberger, Physica A **214** (1995) 547.
- [33] U. Ritschel and H. W. Diehl, Phys. Rev. E **51** (1995) 5392.

- [34] G. Gompper, Z. Phys. B **56** (1984) 217.
- [35] See e.g. J. F. Cardy, *Finite Size Scaling*, (North-Holland, Amsterdam, 1988) for an overview.
- [36] M. H. Fisher and P.-G. de Gennes, C. R. Acad. Sci. Ser. B **287** (1978) 207.
- [37] K. Binder and D. W. Heermann, *Monte Carlo Simulation in Statistical Physics*, (Springer, Berlin, 1988).
- [38] R. H. Swendsen and J.-S. Wang, Phys. Rev. Lett. **58** (1987) 86.
- [39] We adopted the terminology of W. Janke and S. Kappler, Phys. Rev. Lett. **74** (1995) 212.
- [40] J.-S. Wang, Physica A **161** (1989) 249.
- [41] A. Ciach, A. Marciolek, and J. Stecki, *Critical Adsorption in the Undersaturated Regime - Scaling and Exact Results in Ising Strip*, Warsaw preprint (1996).